Cancer Science
Japanese Cancer Association JCA
Open Access

miR-203 inhibits cell proliferation, invasion, and migration of non-small-cell lung cancer by downregulating RGS17

Yongbin Chi,[1] Qinqin Jin,[2] Xinghui Liu,[1] Limin Xu,[1] Xiaoxue He,[1] Yan Shen,[1] Qiang Zhou,[1] Jue Zhang[3] and Mingming Jin[2]

[1]Medical Laboratory; [2]Department of Emergency Medicine, Shanghai Pudong New Area Gongli Hospital, The Second Military Medical University; [3]Clinical Laboratory, Shuguang Hospital Affiliated to Shanghai University of Traditional Chinese Medicine, Shanghai, China

Key words

Invasion and migration, lung cancer, miR-203, proliferation, RGS17

Correspondence

Mingming Jin, Department of Emergency Medicine, Shanghai Gongli Hospital, Second Military Medical University, 219 Miao-Pu Road, Shanghai 200135, China.
Tel: +86-021-5885 8730; Fax: +86-021-5885 8730;
E-mail: asdjinmingming@126.com
and
Jue Zhang, Clinical Laboratory, Shuguang Hospital Affiliated to Shanghai University of Traditional Chinese Medicine, 185 Pu-An Road, Shanghai 200021, China.Tel: +86-021-2025 6557; Fax: +86-021-2025 6557;
E-mail: zhangjue425@hotmail.com

Funding Information

Shanghai Municipal Natural Science Foundation, (Grant/Award Number: '13ZR1437100') Key Discipline Construction project of Pudong Health Bureau of Shanghai (Grant/Award Number: 'PWZx2014-03').

Received August 2, 2017; Revised September 11, 2017; Accepted September 12, 2017

Cancer Sci **108** (2017) 2366–2372

doi: 10.1111/cas.13401

Involvement of the *RGS17* oncogene in the promotion of non-small-cell lung cancer (NSCLC) has been reported, but the regulation mechanism in NSCLC remains unclear. MicroRNAs (miRNAs) negatively regulate gene expression, and their dysregulation has been implicated in tumorigenesis. To understand the role of miRNAs in Regulator of G Protein Signaling 17 (RGS17)-induced NSCLC, we showed that miR-203 was downregulated during tumorigenesis, and inhibited the proliferation and invasion of lung cancer cells. We then determined whether miR-203 regulated NSCLC by targeting RGS17. To characterize the regulatory effect of miR-203 on RGS17, we used lung cancer cell lines, A549 and Calu-1, and the constructed miR-203 and RGS17 overexpression vectors. The CCK8 kit was used to determine cell proliferation, and the Transwell® assay was used to measure cell invasion and migration. RT-PCR, western blots, and immunofluorescence were used to analyze expression of miR-203 and RGS17, and the luciferase reporter assay was used to examine the interaction between miR-203 and RGS17. Nude mice were used to characterize *in vivo* tumor growth regulation. Expression of miR-203 inhibited proliferation, invasion, and migration of lung cancer cell lines A549 and Calu-1 by targeting RGS17. The regulatory effect of miR-203 was inhibited after overexpression of RGS17. The luciferase reporter assay showed that miR-203 downregulated RGS17 by direct integration into the 3′-UTR of RGS17 mRNA. *In vivo* studies showed that expression of miR-203 significantly inhibited growth of tumors. Taken together, the results suggested that expression of miR-203 inhibited tumor growth and metastasis by targeting RGS17.

Morbidity and mortality of lung cancer have recently increased.[1,2] Currently, lung cancer is the leading cause of human mortality from cancer. Recent studies have reported that the Regulator of G Protein Signaling 17 (*RGS17*), located on chromosome 6q25.3,[3,4] codes for a member of the RZ family of RGS proteins that has been frequently reported to be overexpressed in human lung adenocarcinoma, prostate cancer, breast cancer, and hepatocellular carcinoma.[5–7] Furthermore, increased RGS17 protein expression has been positively correlated with tumor cell proliferation by the cyclic AMP-PKA-CREB pathway in human lung and prostate cancers. Thus, RGS17 is regarded as a possible therapeutic target for lung and prostate cancer treatment,[8,9] and these results suggest a potentially important role of RGS17 in oncogenesis.

MicroRNAs (miRNAs) are small non-coding RNAs that regulate a variety of biological processes by modulating gene expression at the post-transcriptional level.[10] Increasing evidence suggests that miRNAs play an important role in the control of cancer cell invasion and metastasis.[11–13] For example, miR-19 triggers the epithelial–mesenchymal transition of lung cancer cells, which is accompanied by growth inhibition.[14] miR-92a promotes the epithelial–mesenchymal transition through activation of the PTEN/PI3K/AKT signaling pathway in non-small-cell lung cancer (NSCLC) metastasis.[15] In the present study, we found that low expression of miR-203 was indicative of NSCLC, and miR-203 expression was negatively correlated with lymphatic metastasis.[16] Increased expression of miR-203 suppressed tumor growth, migration, and invasion of NSCLC cells.[17–19] Using a combination of bioinformatics and functional analyses (http://www.genecards.org/), we found that miR-203 integrated with the 3-'UTR of RGS17 mRNA. In this study, we investigated whether the miR-203-RGS17 interaction inhibited lung cancer progress, and found that increased miR-203 expression significantly reversed RGS17-induced lung cancer cell migration, invasion, and proliferation. In addition, we identified miR-203 as a

regulator that inhibits the expression of RGS17 in lung cancer cell lines.

Materials and Methods

Ethics statement. All animals were treated in accordance with the Guide for the Care and Use of Laboratory Animals, and all experiments were approved and carried out according to the guidelines of the Ethics Committee of Pudong New Area Gongli Hospital, Shanghai, China. All surgical procedures were done under anesthesia, and every effort was made to minimize suffering. Rats were anesthetized by i.p. injection of sodium pentobarbital (30 mg/kg).

Cells lines and cell culture. A549, Calu-1, and HEK293T cells were obtained from the American Type Culture Collection (Manassas, VA, USA). A549 and Calu-1 cells were cultured in RPMI-1640 (Invitrogen, Carlsbad, CA, USA), and HEK293T cells were cultured in DMEM (Invitrogen) supplemented with 10% FBS (Invitrogen) at 37°C in 5% CO_2.

Cell proliferation assays. We determined the effects of miR-203 on GPS17-mediated A549 and Calu-1 cell proliferation. A549 and Calu-1 cells, which were transfected with/without the miR-203 or GPS17 overexpression vector, were seeded onto six 96-well plates at a density of 2×10^3 cells per well. Absorption of cells at different time points was measured at 450 nm using an ELISA reader (Thermo Labsystems, Helsinki, Finland) and using a CCK8 kit (Dojindo Laboratories, Kumamoto, Japan) according to the manufacturer's instructions. Results were representative of at least three separate experiments with three replications per experiment.

Boyden chamber assay. A migration assay was carried out using a Boyden chamber (8 μm; Corning, Corning, NY, USA) containing a polycarbonate membrane. For the invasion assay, 60 μL Matrigel® (BD Biosciences, Franklin Lakes, NJ, USA) was used to mimic the basement membrane. Briefly, 100 μL of 1×10^6 cells in serum-free medium was added to the upper chamber and 600 μL appropriate medium with 10% FBS was added to the lower chamber. Cells were incubated for 24 h. Migratory cells on the under surface of the random regions were fixed and stained with crystal violet for 30 s at room temperature. Photographs of five random regions were taken and number of cells was counted to calculate the average number of migrated cells per plate.

Transfection of cells with the miR-203 mimics vector or the RGS17 overexpression vector. For miR-203 overexpression, the miR-203 mimic or corresponding negative control (miR-NC) was purchased from GenePharma (Shanghai, China). A549 and Calu-1 cells were transfected with either the miR-203 mimic or miR-NC at a final concentration of 50 nM using Lipofectamine® 2000 (Invitrogen) according to the manufacturer's protocol. Cells were used for miR-203 expression analysis or other experiments after 48 h of transfection. For miR-203 inhibition, both A549 and Calu-1 cells were treated with miR-203 inhibitor (Invitrogen) for 48 h, then the effect of miR-203 on RGS17 expression was detected.

For overexpression of RGS17, human RGS17 cDNA with 3-'UTR was cloned into the pMSCV-hygro vector. Primers corresponded to the NCBI Reference Sequence (AF202257.3), and involved the following: forward, 5′-CAGAGCTCATGCGAAAAAGGCAG-3′ and reverse, 5′-GGTCTAGATAAATGAACATTAAG-3′. RGS17 cDNA was inserted into a pMD18-T Simple Vector (Takara, Otsu, Japan) to form the pMD18-T-RGS17 vector. Following sequencing, the recombinant segment of the correct clone was incised by *Bam*HI and *Xba*I (Takara). The recombinant segment was inserted into pMSCV-hygro, which was incised by the same two restriction endonucleases. The pMSCV-hygro-RGS17 clones were sequenced and the correct clones were amplified and identified by restriction enzyme digestion.

The day before transfection, approximately 1×10^6 A549 or Calu-1 cells were seeded in media onto a 60-mm dish and incubated for 24 h. The next day, the cells were transfected using the Sofast gene transfection reagent kit (Sunma, Xiamen, China) according to the manufacturer's instructions. The transfected cells were selected using G418 for 3–4 weeks for subsequent experiments. Monoclonal cells were then cloned and screened for RGS17 expression.

Real-time quantitative PCR (RT-PCR) for detection of miR-203. Total RNA was isolated using TRIzol® reagent (Invitrogen). Reverse transcription was carried out using the RT-PCR system (Promega, Shanghai, China). RT-PCR was carried out in a 20-μL final reaction volume using SYBR® Green I Supermix (Takara, Dalian, China) according to the manufacturer's protocol. All reactions were run in triplicate on an iCycler IQ Multicolor Detection System (Bio-Rad, Hercules, CA, USA) with the following cycling parameters: 95°C for 10 s followed by 40 cycles of 94°C for 15 s, annealing at 55°C for 30 s, and a final extension at 70°C for 30 s. All quantitations were normalized to the level of human U6 snRNA in the reaction. The comparative threshold cycle (CT) ($2^{-\Delta\Delta Ct}$) method, which compares differences in CT values between common reference RNA and target gene RNA, was used to obtain the relative fold changes in gene expression. The miR-203 and RGS17 primers for PCR were designed by GenePharma (Shanghai, China). Results are expressed as mean ± standard error (SE).

Luciferase reporter assay. To construct luciferase reporter vectors, the 3′-UTR of RGS17 cDNA fragments containing the predicted potential miR-203 binding sites were amplified by PCR and subcloned downstream of the luciferase gene in the PYr-MirTarget luciferase vector (Ambion, Austin, TX, USA). The 3′-UTR of RGS17 (containing the binding sites for miR-203) was amplified from a cDNA library with the following primers: forward, 5′-CTCGAGGTA**ACAATGGTATTCAACATTCTAT**ATAC-3′ and reverse, 5′-GCGGCCGCTGCCACAGTTTTGGCAGTGAAC-3′. The mutant 3′-UTR of RGS17 (in which 10 nucleotides were mutated in the binding sites) was amplified using the following primer sequences: forward, 5′-CTCGAGGTA**ACAA*ACCA*ATTC*TTACAA*CTAT**ATAC-3′ and reverse, 5′-GCGGCCGCTGCCACAGTTTTGGCAGTGAAC-3′.

For luciferase assays, HEK293T cells were cultured in 24-well plates and cotransfected with 50 ng of the corresponding vectors containing firefly luciferase together with 25 ng miR-203 or the control. Transfection was carried out using Lipofectamine® 2000 reagent (Invitrogen). At 48 h post-transfection, the relative luciferase activity was calculated by normalizing the firefly luminescence to the Renilla luminescence using the Dual-Luciferase Reporter Assay (Promega, Madison, WI, USA) according to the manufacturer's instructions.

***In vivo* studies.** Animal studies were carried out according to institutional guidelines. A549 cells were stably infected with/without the miR-203 overexpression mimic vectors. A total of 5×10^6 viable cells were injected into the right flanks of nude mice. Tumor sizes were measured using a vernier caliper every 5 days, and tumor volume was calculated using the formula: volume = 1/2 × length × width^2. At 30 days after

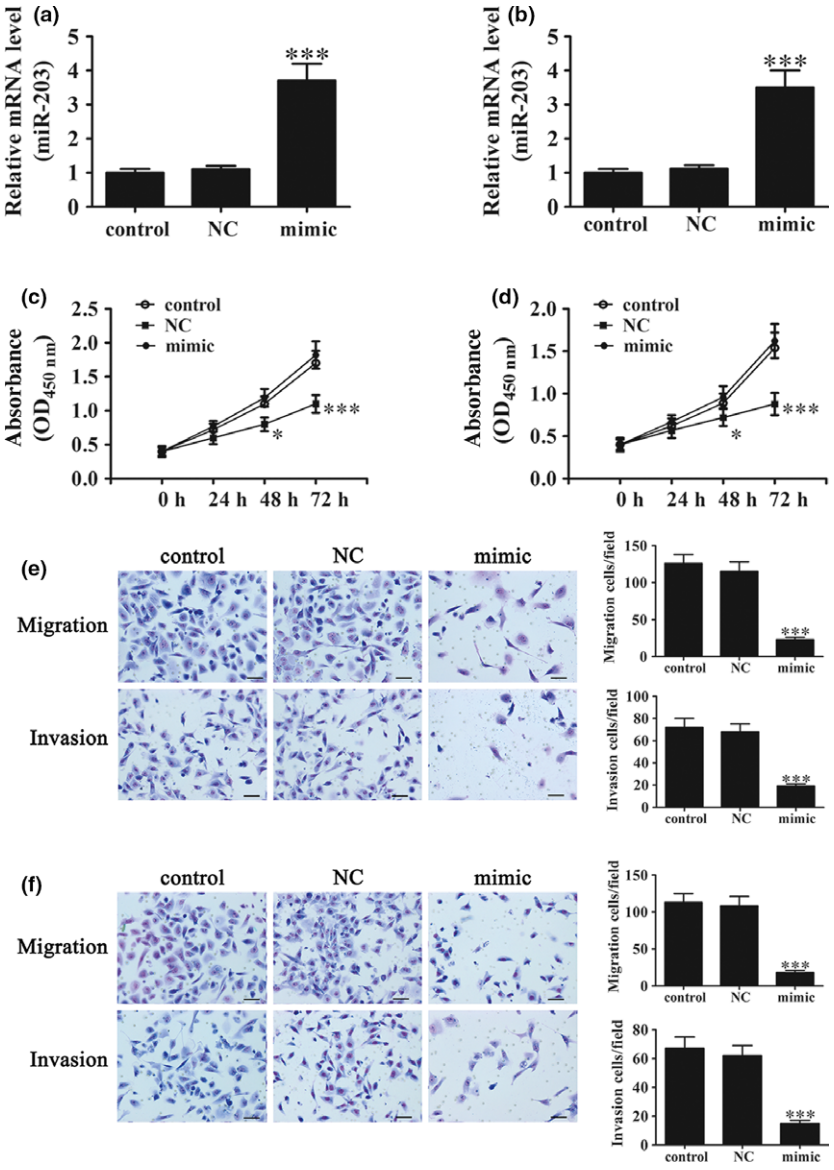

Fig. 1. Micro RNA (miR)-203 overexpression significantly inhibited cell proliferation, migration, and invasion. (a, b) Expression level of miR-203 in (a) A549 and (b) Calu-1 cells was measured using quantitative RT-PCR after transfection with the miR-203 mimic or corresponding negative control (miR-NC). Data are expressed as mean ± SD, $n = 5$. $^{*}P < 0.05$, $^{***}P < 0.001$ *vs* control. (c, d) Ectopic expression of miR-203 significantly inhibited (c) A549 and (d) Calu-1 cell proliferation. (e) Cell migration and invasion were determined in A549 cells using the Transwell (Costar, Cambridge, MA, USA) assay after transfection with the miR-203 mimic or miR-NC. Scale bar, 20 μm. Data are expressed as mean ± SD. $^{***}P < 0.001$ *vs* control. (f) Cell migration and invasion were determined in Calu-1 cells using the Transwell® assay after transfection with the miR-203 mimic or miR-NC. Scale bar, 20 μm. Data are expressed as mean ± SD. $^{***}P < 0.001$ *vs* control.

implantation, the mice were killed, tumors dissected, and tumor weights were measured.

Western blot analysis. Protein was extracted from tissues and cells using RIPA lysis buffer containing proteinase inhibitor (Sigma-Aldrich, St Louis, MO, USA). Protein concentration was determined using the BCA Protein Assay Kit (Vigorous Biotechnology Beijing, Beijing, China). Equal amounts of protein lysates (20 μg each lane) were resolved using 10% SDS-PAGE gels, and then electroblotted onto nitrocellulose membranes (Millipore, Madison, WI, USA). The membranes were blocked for 2 h with 5% non-fat dry milk in Tris-buffered saline containing 0.1% Tween-20, and incubated at 4°C overnight with the following primary antibodies: mouse monoclonal anti-human IRS-1 (1:1000; Santa Cruz Biotechnology, Santa Cruz, CA, USA), mouse monoclonal anti-human RGS-17 (1:500; Santa Cruz Biotechnology), and mouse monoclonal anti-human GAPDH (1:5000; Santa Cruz Biotechnology). GAPDH was used as an internal control for protein loading. The membrane was further incubated with HRP-conjugated goat anti-mouse IgG (1:5000; Santa Cruz Biotechnology) for 1 h at room temperature. Immune complexes were detected by ECL (Cell Signaling Technology, Danvers, MA, USA). Integrated density of the band was quantified by Quantity One software (Bio-Rad).

Immunofluorescence. Cells were incubated with RGS17 antibodies at 4°C overnight, then incubated with conjugated secondary antibody for 1 h at room temperature in the dark. After several washes with PBS, slides were incubated with DAPI for 3 min and then mounted in glycerol. Fluorescence was assessed under a fluorescence microscope.

Statistical analysis. Continuous variables were expressed as mean ± standard deviation (SD). One-way ANOVA was carried out for multiple comparisons using GraphPad Prism software, version 5.0 (GraphPad, La Jolla, CA, USA). *P*-values ≤0.05 indicated a statistically significant difference.

Results

MiR-203 inhibited tumorigenicity and metastasis *in vivo*. In order to identify the effect of miR-203 on lung cell proliferation, migration, and invasion, both A549 and Calu-1 cells were transfected with the miR-203 overexpression mimic vector.

After 48 h of transfection, expression level of miR-203 was detected by RT-PCR. Result showed that the expression of miR-203 was significantly increased (3.5-fold upregulated) in both A549 and Calu-1 cells compared with the control group (Fig. 1a,b). Cell proliferation was then determined using a cell-counting kit, with 2×10^3 cells used as the initial concentration. After culturing for different times (0, 24, 48, and 72 h), cell proliferation was detected by measuring the absorbance at 450 nm. Expression of miR-203 significantly suppressed cell proliferation at 48 h in both A549 and Calu-1 cells. However, there was no significant difference after transfection with the miR-203-NC vector compared with the control group (Fig. 1c,d). To determine the effect of miR-203 on metastasis, Transwell (Costar) migration and invasion assays were carried out using A549 and Calu-1 cells transfected with the miR-203 mimic, miR-203-NC, or their respective controls. The miR-203-transfected lung cells showed significantly lower migration and invasiveness than the control or miR-203-NC group when using the Boyden Transwell® assay (Fig. 1e,f). Together, these results showed that miR-203 inhibited lung cancer cell proliferation, migration, and invasion *in vitro*.

RGS-17 overexpression reversed miR-203-induced cell proliferation, migration, and invasion inhibition. Previous studies showed that RGS17 expression played an important role in the maintenance of tumor cell proliferation.[8] To determine whether RGS17 was involved in the suppression of miR-203-mediated tumor cell proliferation, the RGS17 overexpression vector was constructed and successfully transfected into A549 and Calu-1 cells. Western blots showed that the expression of RGS17 was significantly increased in both A549 and Calu-1 cells (Fig. 2a,b). Previous studies reported that the expression of miR-203 significantly inhibited proliferation of both A549 and Calu-1 cells. However, RGS17 overexpression reversed miR-203-induced proliferation inhibition in both A549 and Calu-1 cells (Fig. 2c,d). Transwell® migration and invasion assays were carried out using A549 and Calu-1 cells, showing that RGS17-transfected lung cells significantly reversed the miR-203-induced migration and invasiveness inhibition using the Boyden Transwell® assay (Fig. 2e,f). Taken together, the result showed that the antitumor effect of miR-203 on lung cancer cells was decreased after overexpression of RGS17.

RGS-17 was the direct target of miR-203. To determine the possible interaction between miR-203 and RGS-17, we first carried out a bioinformatics screen for its possible target genes, using an online 3′-UTR binding site prediction database (http://www.genecards.org/). A total of 58 miRNAs were

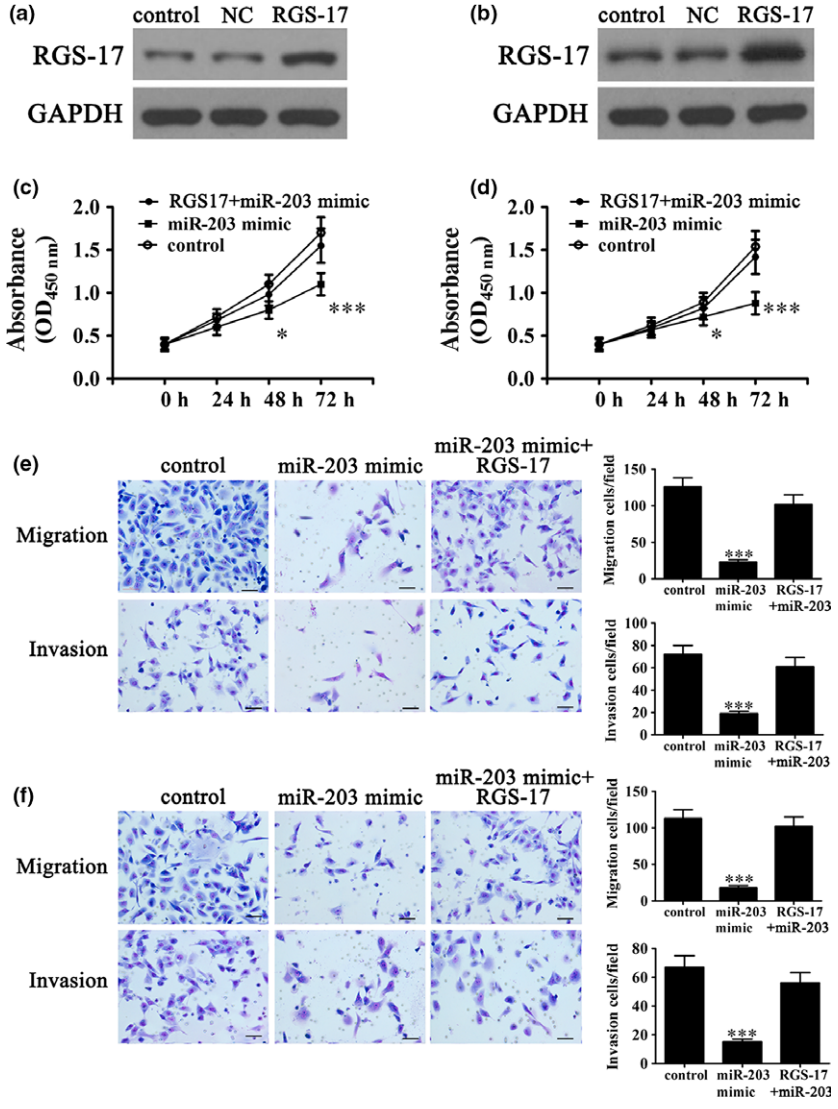

Fig. 2. Expression of RGS-17 decreased micro RNA (miR)-203-induced cell proliferation, migration, and invasion. (a, b) Western blot analysis shows the expression of RGS-17 in (a) A549 and (b) Calu-1 cells after transfection with the RGS-17 overexpression vector or the corresponding negative control (NC) vector. (c, d) Ectopic expression of RGS-17 significantly reversed miR-203-induced (c) A549 and (d) Calu-1 cell proliferation suppression. Data are expressed as mean ± SD. $^*P < 0.05$, $^{***}P < 0.001$ *vs* control. (e) Cell migration and invasion were determined in A549 cells using the Transwell (Costar) assay. Scale bar, 20 μm. Data are expressed as mean ± SD. $^{***}P < 0.001$ *vs* control. (f) Cell migration and invasion were determined in Calu-1 cells using the Transwell® assay. Scale bar, 20 μm. Data are expressed as mean ± SD. $^{***}P < 0.001$ *vs* control.

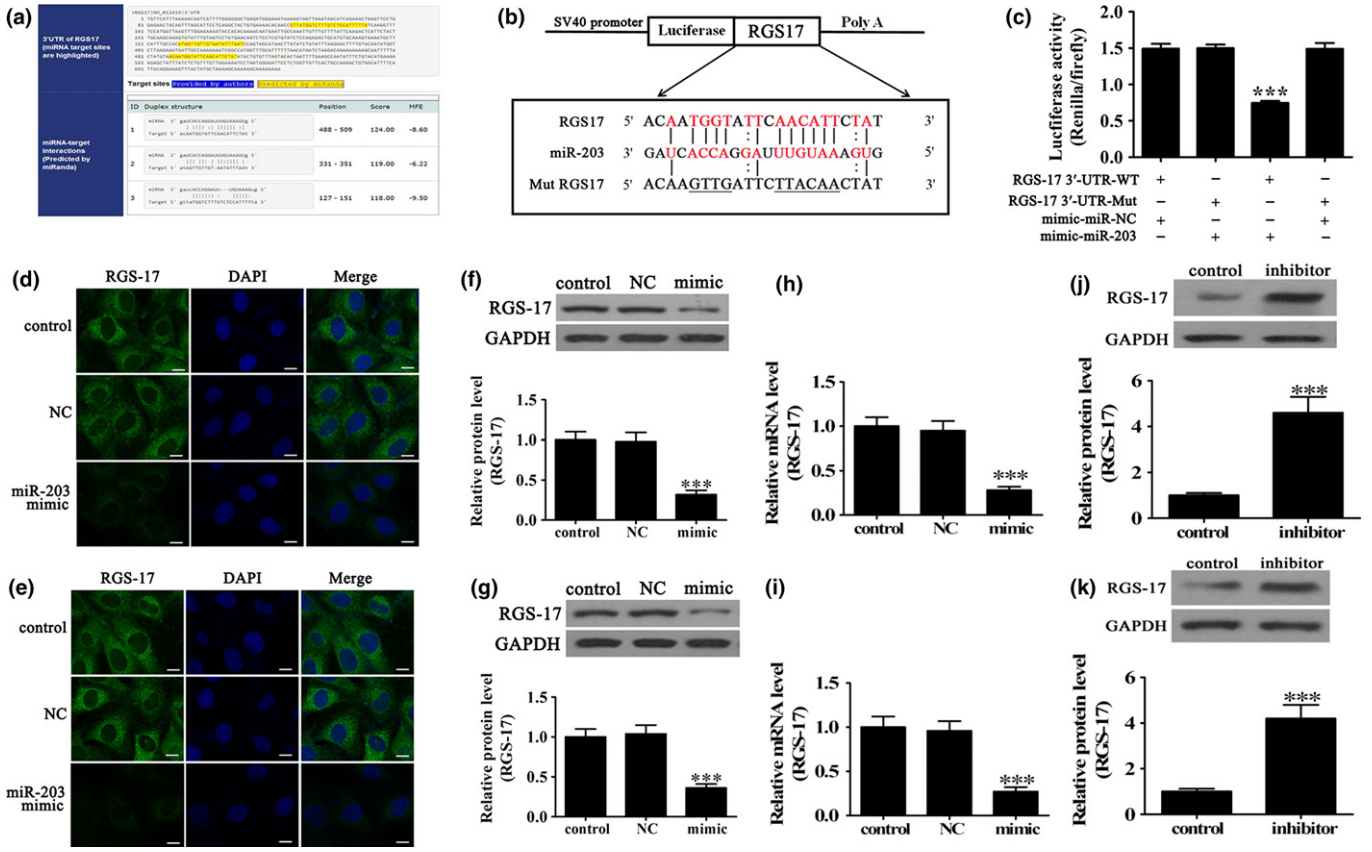

Fig. 3. RGS-17 is a potential target of micro RNA (miR)-203. (a, b) Complementary sequences between miR-203 and the 3′-UTR of RGS-17 mRNA were obtained using publicly available algorithms. The mutated version of the RGS-17 3′-UTR is also shown. (c) The 3′-UTR of RGS-17 was fused to the luciferase coding region (PYr-RGS-17 3′-UTR) and cotransfected into HEK293T cells with miR-203 mimics to confirm that RGS-17 is the target of miR-203. PYr-RGS-17 3′-UTR and miR-203 mimic constructs were cotransfected into HEK293T cells with a control vector and relative luciferase activity was determined 48 h after transfection. Data are expressed as mean ± SD. ***$P < 0.001$ *vs* control. (d, e) Representative images of the immunofluorescent staining of RGS-17 in (d) A549 and (e) Calu-1 cells. Scale bar, 5 μm. (f, g) Western blot analysis of the effect of RGS-17 expression in (f) A549 and (g) Calu-1 cells after transfection with miR-203 mimics ($n = 5$). GAPDH expression levels were detected as an endogenous control. Data are expressed as mean ± SD. ***$P < 0.001$ *vs* control. (h,i) RT-PCR analysis of the effect of RGS-17 expression in (h) A549 and (i) Calu-1 cells after transfection with miR-203 mimics ($n = 5$). GAPDH expression levels were detected as an endogenous control. Data are expressed as mean ± SD. ***$P < 0.001$ *vs* control. (j, k) Western blot analysis of the effect of RGS-17 expression in (j) A549 and (k) Calu-1 cells after treatment with miR-203 inhibitor ($n = 5$). GAPDH expression levels were detected as an endogenous control. Data are expressed as mean ± SD. ***$P < 0.001$ *vs* control.

predicted to target RGS-17 (Fig. 3a). Overlap analyses showed that miR-203 had a broadly conserved binding site. A mutated version of the RGS-17 3′-UTR was constructed in which 10 complementary nucleotides in the binding site were altered (Fig. 3b). This mutated construct was fused to the luciferase-coding region (PYr-RGS-17 3′-UTR) and co-transfected into HEK293T cells along with miR-203 mimics (Fig. 3c). The relative luciferase activity showed that when the wild-type RGS-17 3′-UTR was cotransfected with miR-203 mimics, RGS-17 expression was significantly decreased ($P < 0.001$) compared with cotransfection with the control miRNA. However, this effect was not observed after mutant 3′-UTR of RGS-17, indicating that miR-203 can specific suppression RGS-17 expression by targeting 3′-UTR of RGS-17.

Immunofluorescent analyses were then used to determine the expression level of RGS-17 after transfection with miR-203 mimic or miR-203-NC. The results showed that expression of RGS-17 was significantly suppressed in both A549 and Calu-1 cells after miR-203 overexpression (Fig. 3f–i). Western blot and RT-PCR analyses further confirmed that miR-203 expression significantly inhibited RGS-17 expression in both protein and mRNA level *in vitro* (Fig. 3f,g). Our result also showed that inhibiting miR-203 expression with mir-203 inhibitor treatment significantly promoted RGS-17 expression in both A549 and Calu-1 cells (Fig. 3j,k).

miR-203 expression inhibited tumor growth *in vivo*. After showing that overexpression of miR-203 played an important role in inhibiting lung cancer cell growth *in vitro*, we determined whether miR-203 had a similar antitumor effect *in vivo*. A549 cells stably expressing miR-NC or miR-203 were s.c. inoculated into nude mice ($n = 6$ for each group). Size of A549 tumors in the mice was measured using a caliper every 5 days. Results showed that tumor volume was significantly decreased in the group treated with the miR-203 mimic compared with the control and miR-NC groups (Fig. 4a). The tumors were extracted after implantation for 30 days, and tumor weight of the miR-203 mimic group was significantly lower compared to the control and miR-NC groups (Fig. 4b,c). miR-203 expression in xenograft tumors was then determined using quantitative RT-PCR. Results showed that miR-203 expression was upregulated in the xenograft tumors from the miR-203 mimic group compared to the xenograft tumors of

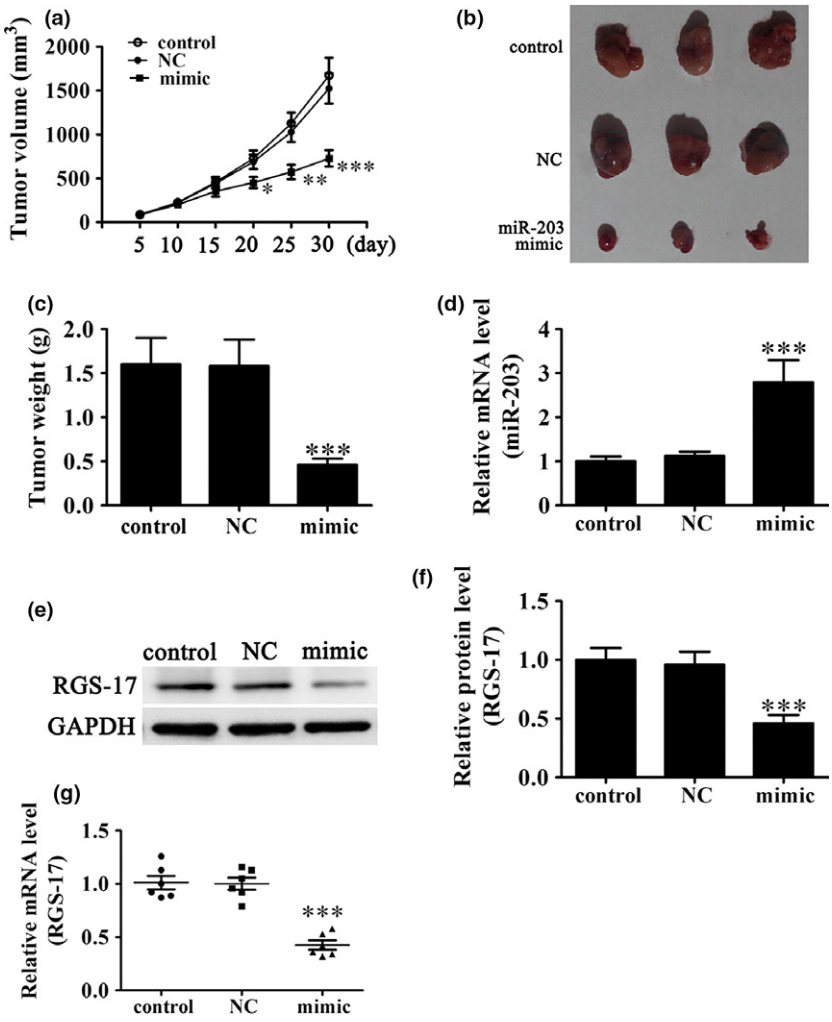

Fig. 4. Micro RNA (miR)-203 suppressed tumor growth of lung cancer in a xenograft model. (a) Growth curves of tumor volumes in xenografts of nude mice were determined based on tumor volume measured every 5 days for 30 days ($n = 6$). $^*P < 0.05$, $^{**}P < 0.01$, $^{***}P < 0.001$ *vs* control group. (b) Photographs of tumor tissues from different groups at day 30. (c) Tumor weights of different groups at day 30 ($n = 6$). $^{***}P < 0.001$ *vs* control group. (d) Expression of miR-203 was detected by quantitative RT-PCR ($n = 6$). Data are expressed as mean ± SD. $^{***}P < 0.001$ *vs* control group. (e, f) RGS-17 level in tumor tissues of different groups was determined by western blot analyses. Data are expressed as mean ± SD. $^{***}P < 0.001$ *vs* control group. (g) The mRNA level of RGS-17 in tumor tissues of different groups was determined by RT-PCR analyses. Data are expressed as mean ± SD. $^{***}P < 0.001$ *vs* control group.

the miR-NC and control groups (Fig. 4d). Western blot and RT-PCR analyses showed that RGS-17 protein levels and mRNA level were significantly decreased in the miR-203 mimic group compared with the control and miR-NC groups (Fig. 4e–g). Taken together, the results show that upregulation the expression of miR-203 suppressed lung tumor growth by inhibit RGS-17 in mRNA level.

Discussion

An increasing number of studies have reported that miR-203 is frequently downregulated in numerous types of cancer cells, such as osteosarcoma,[20] colorectal cancer,[21] hepatocellular carcinoma,[22] breast cancer,[23] and NSCLC[24] cells. Changes in the expression of miR-203 results in antitumor effects, suggesting that miR-203 plays an important role in regulating tumorigenesis. Thus, investigating the mechanisms underlying the involvement of miR-203 in different types of cancer may have important clinical implications.

In contrast to miR-203, the expression of RGS-17 induces tumorigenesis. Recently, there are some studies showing that the expression of RGS-17 is upregulated and promotes tumor growth and migration in human colorectal carcinoma. RGS17 is one of the smallest RGS proteins, and lacks well-defined functional domains outside of the RGS domain. RGS17 is a member of the RZ (A) subfamily of RGS proteins and preferentially deactivates members of the G_i/G_o family of G-proteins.[25,26] RGS17 also contains a palmitoylation site that is located at the N-terminal region of the RGS domain. This site potentially regulates its subcellular localization, further affecting G-protein and receptor selectivity. In contrast to miR-203, clinical expression data available in the Oncomine database suggest that the expression of RGS17 is regulated in carcinoma cells, such as in hepatocellular carcinoma,[26] lung cancer, and prostate cancer.[8,27] Expression of RGS-17 increases proliferation, migration, and invasion, and even promotes resistance to chemotherapy of tumors. Investigating the mechanisms of how to regulate RGS17-mediated tumor metabolism may therefore have important clinical implications.

In the present study, we found that expression of miR-203 significantly suppressed NSCLC cell growth, and decreased cell migration and invasion as reported in previous studies.[18,19,24,28,29] However, overexpression of RGS17 reversed the miR-203-induced antitumor effect. The bifluorescein test further verified that miR-203 integrated into the 3′-UTR of RGS-17 and post-transcriptionally downregulated RGS-17 expression. We also showed that miR-203 inhibited cell proliferation, invasion, and migration of NSCLC by downregulating RGS17. However, the exact regulatory mechanism of RGS-17 promotion of cell proliferation, invasion, and migration of NSCLC is still unknown and needs further study.

In conclusion, the present study showed that miR-203 inhibited cell proliferation, invasion, and migration in NSCLC by targeting the 3′-UTR of RGS-17. miR-203 may therefore be a novel diagnostic and therapeutic option for the treatment of patients with NSCLC.

Disclosure Statement

Authors declare no conflicts of interest for this article.

Acknowledgments

This work was funded by grants from the Shanghai Municipal Natural Science Foundation (No. 13ZR1437100), Key Discipline Construction project of Pudong Health Bureau of Shanghai (No. PWZx2014-03).

References

1 Shash E, Peccatori FA, Azim HA Jr. Optimizing the use of epidermal growth factor receptor inhibitors in advanced non-small-lung cancer (NSCLC). *J Thorac Dis* 2011; **3**: 57–64.
2 Lim JS, Ibaseta A, Fischer MM *et al.* Intratumoural heterogeneity generated by Notch signalling promotes small-cell lung cancer. *Nature* 2017; **545**: 360–4.
3 Rangel J, Nosrati M, Leong SP *et al.* Novel role for RGS1 in melanoma progression. *Am J Surg Pathol* 2008; **32**: 1207–12.
4 Sierra DA, Gilbert DJ, Householder D *et al.* Evolution of the regulators of G-protein signaling multigene family in mouse and human. *Genomics* 2002; **79**: 177–85.
5 Hurst JH, Hooks SB. Regulator of G-protein signaling (RGS) proteins in cancer biology. *Biochem Pharmacol* 2009; **78**: 1289–97.
6 Sokolov E, Iannitti DA, Schrum LW, McKillop IH. Altered expression and function of regulator of G-protein signaling-17 (RGS17) in hepatocellular carcinoma. *Cell Signal* 2011; **23**: 1603–10.
7 Li Y, Li L, Lin J *et al.* Deregulation of RGS17 expression promotes breast cancer progression. *J Cancer* 2015; **6**: 767–75.
8 James MA, Lu Y, Liu Y, Vikis HG, You M. RGS17, an overexpressed gene in human lung and prostate cancer, induces tumor cell proliferation through the cyclic AMP-PKA-CREB pathway. *Cancer Res* 2009; **69**: 2108–16.
9 Bodle CR, Mackie DI, Roman DL. RGS17: an emerging therapeutic target for lung and prostate cancers. *Future Med Chem* 2013; **5**: 995–1007.
10 Bartel DP. MicroRNAs: genomics, biogenesis, mechanism, and function. *Cell* 2004; **116**: 281–97.
11 Nicoloso MS, Spizzo R, Shimizu M, Rossi S, Calin GA. MicroRNAs–the micro steering wheel of tumour metastases. *Nat Rev Cancer* 2009; **9**: 293–302.
12 Sheervalilou R, Shirvaliloo S, Fekri Aval S *et al.* A new insight on reciprocal relationship between microRNA expression and epigenetic modifications in human lung cancer. *Tumour Biol* 2017; **39**: 1010428317695032.
13 Li Z, Yu X, Shen J, Law PT, Chan MT, Wu WK. MicroRNA expression and its implications for diagnosis and therapy of gallbladder cancer. *Oncotarget* 2015; **6**: 13914–21.
14 Li J, Yang S, Yan W *et al.* MicroRNA-19 triggers epithelial-mesenchymal transition of lung cancer cells accompanied by growth inhibition. *Lab Invest* 2015; **95**: 1056–70.
15 Lu C, Shan Z, Hong J, Yang L. MicroRNA-92a promotes epithelial-mesenchymal transition through activation of PTEN/PI3K/AKT signaling pathway in non-small cell lung cancer metastasis. *Int J Oncol* 2017; **51**: 235–44.
16 Tang R, Zhong T, Dang Y, Zhang X, Li P, Chen G. Association between downexpression of MiR-203 and poor prognosis in non-small cell lung cancer patients. *Clin Transl Oncol* 2016; **18**: 360–8.
17 Zhou Y, Liang H, Liao Z *et al.* miR-203 enhances let-7 biogenesis by targeting LIN28B to suppress tumor growth in lung cancer. *Sci Rep* 2017; **7**: 42680.
18 Duan X, Fu Z, Gao L *et al.* Direct interaction between miR-203 and ZEB2 suppresses epithelial-mesenchymal transition signaling and reduces lung adenocarcinoma chemoresistance. *Acta Biochim Biophys Sin (Shanghai)* 2016; **48**: 1042–9.
19 Singh T, Prasad R, Katiyar SK. Therapeutic intervention of silymarin on the migration of non-small cell lung cancer cells is associated with the axis of multiple molecular targets including class 1 HDACs, ZEB1 expression, and restoration of miR-203 and E-cadherin expression. *Am J Cancer Res* 2016; **6**: 1287–301.
20 Lin W, Zhu X, Yang S *et al.* MicroRNA-203 inhibits proliferation and invasion, and promotes apoptosis of osteosarcoma cells by targeting Runt-related transcription factor 2. *Biomed Pharmacother* 2017; **91**: 1075–84.
21 Shen B, Yuan Y, Zhang Y *et al.* Long non-coding RNA FBXL19-AS1 plays oncogenic role in colorectal cancer by sponging miR-203. *Biochem Biophys Res Commun* 2017; **488**: 67–73.
22 Fang JF, Zhao HP, Wang ZF, Zheng SS. Upregulation of RASAL2 promotes proliferation and metastasis, and is targeted by miR-203 in hepatocellular carcinoma. *Mol Med Rep* 2017; **15**: 2720–6.
23 Mohammadzadeh R, Saeid Harouyan M, Ale Taha SM. Silencing of bach1 gene by small interfering RNA-mediation regulates invasive and expression level of miR-203, miR-145, matrix metalloproteinase-9, and CXCR4 receptor in MDA-MB-468 breast cancer cells. *Tumour Biol* 2017; **39**: 1010428317695925.
24 Wang S, Zhu L, Zuo W *et al.* MicroRNA-mediated epigenetic targeting of Survivin significantly enhances the antitumor activity of paclitaxel against non-small cell lung cancer. *Oncotarget* 2016; **7**: 37693–713.
25 Mao H, Zhao Q, Daigle M, Ghahremani MH, Chidiac P, Albert PR. RGS17/RGSZ2, a novel regulator of Gi/o, Gz, and Gq signaling. *J Biol Chem* 2004; **279**: 26314–22.
26 Nunn C, Mao H, Chidiac P, Albert PR. RGS17/RGSZ2 and the RZ/A family of regulators of G-protein signaling. *Semin Cell Dev Biol* 2006; **17**: 390–9.
27 Hooks SB, Callihan P, Altman MK, Hurst JH, Ali MW, Murph MM. Regulators of G-Protein signaling RGS10 and RGS17 regulate chemoresistance in ovarian cancer cells. *Mol Cancer* 2010; **9**: 289.
28 Hu H, Xu Z, Li C *et al.* MiR-145 and miR-203 represses TGF-beta-induced epithelial-mesenchymal transition and invasion by inhibiting SMAD3 in non-small cell lung cancer cells. *Lung Cancer* 2016; **97**: 87–94.
29 Funamizu N, Lacy CR, Kamada M, Yanaga K, Manome Y. MicroRNA-203 induces apoptosis by upregulating Puma expression in colon and lung cancer cells. *Int J Oncol* 2015; **47**: 1981–8.